Plant Molecular Biology (2021) 107:355–364
https://doi.org/10.1007/s11103-020-01115-7

Kleisin NSE4 of the SMC5/6 complex is necessary for DNA double strand break repair, but not for recovery from DNA damage in Physcomitrella (*Physcomitrium patens*)

Marcela Holá[1] · **Radka Vágnerová**[1] · **Karel J. Angelis**[1]

Received: 23 February 2020 / Accepted: 31 December 2020 / Published online: 6 February 2021

Abstract

Key message **Kleisin NSE4 and circular form of SMC5/6 is indispensable for DSB repair and necessary for gene targeting but is not enough for recovery of cells from DNA damage in Physcomitrella.**

Abstract Structural maintenance of chromosomes (SMC) complexes are involved in cohesion, condensation and maintenance of genome stability. Based on the sensitivity of mutants to genotoxic stress the SMC5/6 complex is thought to play a prominent role in DNA stabilization during repair by tethering DNA at the site of lesion by a heteroduplex of SMC5 and SMC6 encircled with non-SMC components NSE1, NSE3 and kleisin NSE4. In this study, we tested how formation of the SMC5/6 circular structure affects mutant sensitivity to DNA damage, kinetics of DSB repair and gene targeting. In the moss Physcomitrella (*Physcomitrium patens*), *SMC6* and *NSE4* are essential single copy genes and this is why we used blocking of transcription to reveal their mutated phenotype. Even slight reduction of transcript levels by dCas9 binding was enough to obtain stable lines with severe DSB repair defects and specific bleomycin sensitivity. We show that survival after bleomycin or MMS treatment fully depends on active SMC6, whereas attenuation of NSE4 has little or negligible effect. We conclude that circularization of SMC5/6 provided by the kleisin NSE4 is indispensable for the DSB repair, nevertheless there are other functions associated with the SMC5/6 complex, which are critical to survive DNA damage.

Keywords *Physcomitrium patens* · Physcomitrella · SMC5/6 complex · NSE4 kleisin · dCas9 · DNA repair · Gene targeting · Comet assay

Introduction

Plants as sessile organisms developed several strategies to protect the integrity of their genomes against various environmental stresses including exposure to mutagens. The bryophyte Physcomitrella (*P. patens*) stands aside from other plants (Rensing et al. 2020) with high frequency of homologous recombination (HR) and remarkable ability to integrate transgenes at predefined loci through homologous recombination-mediated gene targeting (GT) (Kamisugi et al. 2016). Experimentally, *P. patens* is highly amenable to analysis and manipulation e.g. for study of DNA damage and repair by comet assay (Angelis et al. 2015). *P. patens* spore germinates to form a haploid filamentous structure called protonema, composed of two types of cells—chloronema and caulonema. With respect to in vitro cultivation conditions in basal medium enriched with ammonium tartrate (Knight et al. 2002) protonema is almost exclusively composed of chloronemal cells accumulated at the G2/M transition. This unique tissue-specific cell cycle arrest is thought to be behind the uniquely high rate of HR in *P. patens* nuclear DNA (Schween et al. 2003). Protonema filaments grow exclusively by tip growth of their apical cells (Menand et al. 2007). The advantage of using filamentous *P. patens* is that it can be employed either as a culture of dividing cells comprising of 3–7 cell fragments containing an average of 50% of apical cells obtained from protonemal lawns by extensive shearing or as differentiated tissue from 7-days grown protonemata with only 5% of apical cells.

Supplementary Information The online version contains supplementary material available at https://doi.org/10.1007/s11103-020-01115-7.

✉ Karel J. Angelis
karel.angelis@gmail.com

[1] Institute of Experimental Botany, The Czech Academy of Sciences, Na Karlovce 1, 16000 Prague, Czech Republic

Each culture exhibits different kinetics of DNA repair (Goffova et al. 2019; Kamisugi et al. 2012).

Assays based on the activity of the enzyme APT (adenine phosphoribosyltransferase) can be used to distinguish between different DNA repair pathways. APT is an enzyme of the purine salvage pathway that converts adenine into AMP and its loss of function generates plants resistant to toxic adenine analogues e.g. 2-Fluoroadenine (2-FA) (Gaillard et al. 1998). Insertional inactivation of the gene can be employed as selectable marker to identify HR-mediated gene targeting of the APT locus, while analysis of nucleotide-level mutations in the APT locus can be used to estimate mutational consequences of conservative DNA repair failure (Trouiller et al. 2006, 2007).

The SMC6 (structural maintenance of chromosome 6) protein is component of the highly conserved SMC5/6 complex that is composed of SMC5 and SMC6 heterodimer and 6 non-SMC elements NSE1-6. Similarly, to the other SMC complexes of cohesin and condensin, the SMC5-SMC6 heterodimer together with NSE4 kleisin bridge form a circular structure capable of entrapping DNA (Palecek et al. 2006). NSE4 in cooperation with NSE1 and NSE3 forms a subcomplex, which directly or indirectly regulates the ring shape and functions of SMC5/6 complex (Vondrova et al. 2020) and plays an important role in embryo and seed development in plants (Diaz et al. 2019; Li et al. 2017; Zelkowski et al. 2019). This conserved core of the SMC5/6 complex is indispensable for all its functions including essential processes like DNA replication and repair (Diaz and Pecinka 2018; Palecek 2018). *NSE4* and *SMC6* are essential genes in yeast and mammals and their knockout is lethal (Hu et al. 2005; Ju et al. 2013; Lehmann et al. 1995) (Fig. 1). The *Arabidopsis* orthologue *AtSMC6B* (*MIM*) was shown to interfere with DSBs repair by eliminating its rapid phase (Kozak et al. 2009). Because the haploid state of the *P. patens* protonema and indispensability of the SMC5/6 complex do not allow complete depletion of any of the complex subunits we used an attenuated expression approach by specific binding of catalytically dead Cas9 (dCas9) lacking endonucleolytic activity to the desired gene to generate mutants with decreased level of transcripts (Qi et al. 2013). Such mutant plants are still viable, growing and manifesting DNA repair phenotypes.

Materials and methods

Plant material and cultivation

The WT *P. patens* (accession (Hedw.) B.S.G. 'Gransden2004') (Rensing et al. 2008), the *ppku70* and *pprad51-1-2* double mutant (Schaefer et al. 2010) were generated by D. G. Schaefer, Neuchatel University, Switzerland, and F. Nogué, INRA, Paris, France, and kindly provided by F. Nogué. All strains were cultured as 'spot inocula' on BCD agar medium supplemented with 1 mM $CaCl_2$ and 5 mM ammonium tartrate (BCDAT medium), or as lawns of protonema filaments by subculture of homogenized tissue on BCDAT agar overlaid with cellophane in growth chambers with 18/6 h day/night cycle at 22/18 °C (Knight et al. 2002).

One-day-old protonema tissue (1d) for repair experiments was prepared from 1-week-old tissue (7d) scraped from plate, suspended in 8 ml of BCDAT medium, sheared at 10 000 rpm for two, 1-min cycles by a T25 homogenizer (IKA, Germany) and left to recover for 24 h in a cultivation chamber with gentle shaking at 100 rpm. This treatment yielded a suspension of 3–5 cell protonemata filaments, which readily settle for recovery.

Generation and analysis of *PpNSE4* and *PpSMC6* mutants

The vectors for attenuation of *PpNSE4* and *PpSMC6* expression were constructed as expression cassettes of dCas9 driven by the maize ubiquitin promoter, an NPTII selection cassette and specific guide RNA (sgRNA). Construction, transformation and validation of mutated lines is described in Supplementary Methods S1.

Three stable transformants of *ppnse4* and *ppsmc6* were randomly picked and analyzed by quantitative RT-PCR (qRT-PCR) for transcript levels of *NSE4* and *SMC6* (Fig. 2b, e). Total RNA was isolated from 7 days old protonemata with RNeasy Plant Mini Kit (Qiagen), treated with DNaseI (DNA-*free*™ DNA Removal Kit, Thermo Fisher Scientific) and reverse transcribed using qPCRBIO cDNA Synthesis Kit (PCR Biosystems). Diluted cDNA reaction mixtures were used for qRT-PCR analysis using the qPCRBIO SyGreen Mix Lo-ROX (PCR Biosystems) in Stratagene-MX3005P. Analysis was performed for three biological replicas (independently cultivated tissue) and in two technical replicates with Clathrin adapter complex subunit *CAP-50* (Pp3c27_2250V3.1) as a reference gene (Kamisugi et al. 2016). The relative transcript levels of *NSE4* and *SMC6* were calculated by the ΔΔCt method (Pfaffl 2004).

Mutagens, treatments and sensitivity assay

Sensitivity to DNA damage was measured after treatment either with freshly prepared solutions of bleomycin sulphate supplied as Bleomedac inj. (Medac, Hamburg, Germany), or methyl methanesulfonate (MMS) (Sigma-Aldrich) in BCDAT medium. Protonemata were dispersed in liquid BCDAT medium containing bleomycin or MMS and treated for 1 h. After treatment and washing recovered protonemata were inoculated as eight explants per quadrant of a Petri dish with drug-free BCDAT agar without

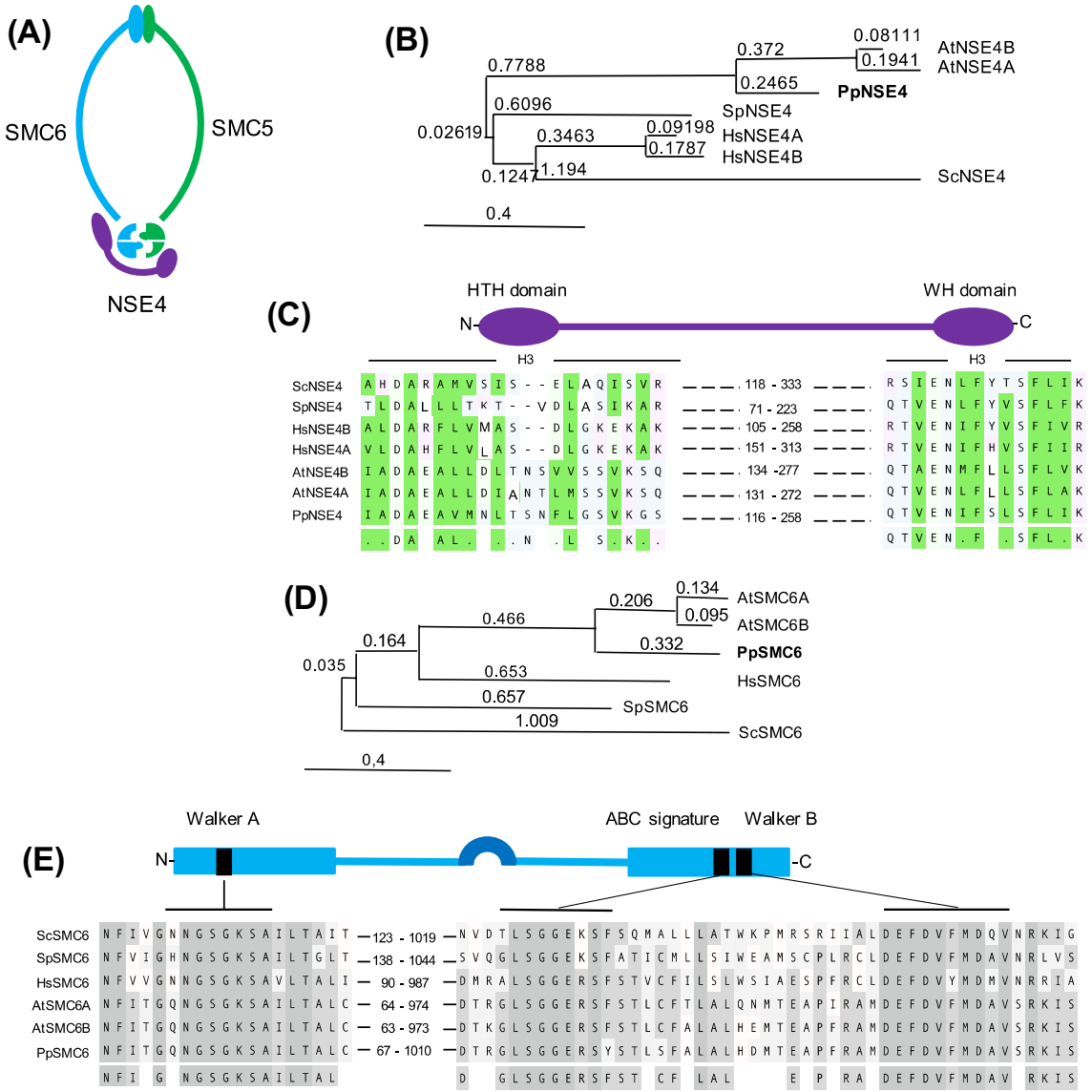

Fig. 1 Structural features of SMC6 and NSE4 proteins and basic characterisation of *P. patens* NSE4 and SMC6 homologs. (**a**) The core structure of SMC5/6 complex formed by SMC5 and SMC6 heterodimer and NSE4 kleisin molecule binding to the SMC6 neck and bridging it to the SMC5 ATPase head via its helix-turn-helix (HTH) and winged helix (WH) domains (Vondrova et al. 2020). (**b**) Midpoint rooted phylogenetic trees of NSE4 and SMC6 (**d**) homologs based on maximum likelihood algorithm. The NSE4 and SMC6 homologs are from *Schizosaccharomyces pombe* (*Sp*), *Saccharomyces cerevisie* (*Sc*), *Homo sapiens* (Hs), *Arabidopsis thaliana* (At) and *Physcomitrium patens* (Pp). (**c**) Arrangement and alignment of the H3 helix from N-terminal HTH and C-terminal WH domains which are critical for NSE4 binging to SMC6 and SMC5, respectively (Palecek et al. 2006; Vondrova et al. 2020). Amino acid green shading represents conserved hydrophobic patterns characteristic for the kleisin family (Schleiffer et al. 2003). (**e**) Arrangement of the conserved ATP-binding motifs in N- and C-terminal domains of SMC6 protein and alignment of the amino acid residues surrounding the Walker A, ABC signature and Walker B nucleotide-binding motifs, forming ATPase domain. In the alignment of SMC6 homologs, the sequences of conserved motifs are marked by black lines. Identical amino acid residues are shaded in grey

cellophane overlay and left to grow. UVC irradiation was performed in a Hoefer UVC 500 crosslinker at 254 nm by irradiating *P. patens* lines spotted as explants on a Petri dish. Irradiation and the following steps were performed for 24 h in the dark or under red illumination to block photolyases. Treatment was assessed after 3 weeks by weighing explants. The fresh weight of the treated explants was normalized to the fresh weight of untreated explants of the same line and plotted as % of 'Relative fresh weight'. In every experiment, the treatment was carried in duplicate and experiments were repeated two or three times and statistically analyzed by Student's *t* test.

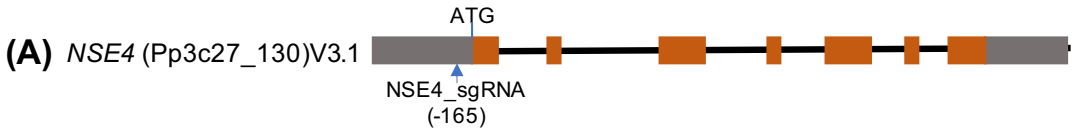

(B)

Genotype	Transcript	SD
WT	1.00	0.03
nse4-2	1.09	0.03
nse4-3	0.91	0.02
nse4-4	0.85	0.01

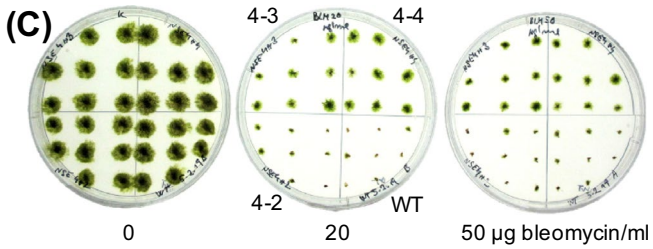

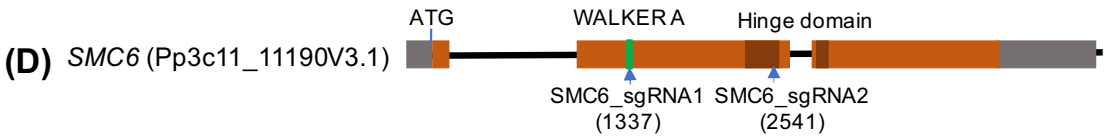

(E)

Genotype	Transcript	SD
WT	1.03	0.05
smc6-3	0.61	0.12
smc6-4	0.71	0.10
smc6-5	0.81	0.07

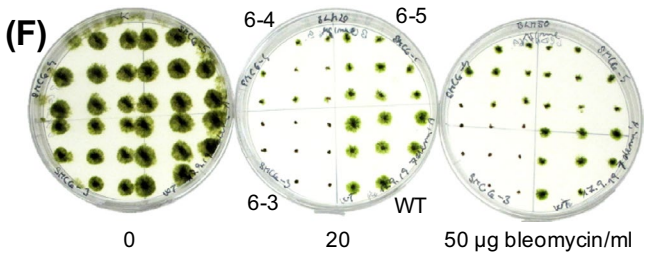

(G)

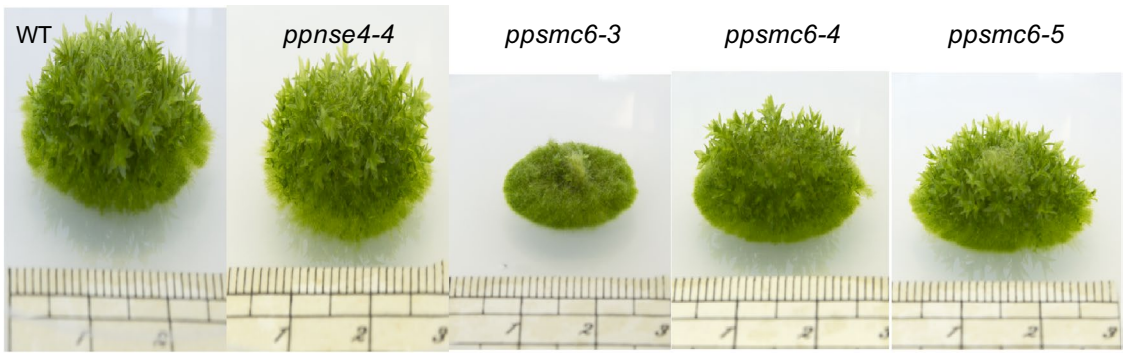

(H)

Genotype	Population	2-FA^R	Rate in 10^5
WT	297271	0	0
nse4-4	327894	0	0
smc6-3	252379	11	6.6

Fig. 2 Characterization of *ppnse4* and *ppsmc6* mutants. Structure of the *PpNSE4* (**a**) and of the *PpSMC6* (**d**) loci with indication of dCas9 binding. The boxes represent exons and the gray shading indicate UTR regions. Relative transcript levels to WT estimated by qRT-PCR of *NSE4* (**b**) and of *SMC6* (**e**) in mutant plants. Primers are listed in Supplementary Table S1. Sensitivity of *nse4* (**c**) and of *smc6* (**f**) plants to 20 and 50 µg/ml of bleomycin treatment. Assignment of mutants to sectors is indicated on the edge of plates with plants treated with 20 µg bleomycin/ml. **g** Morphology of colonies of WT, *ppnes4-4* and *ppsmc6-3*, *ppsmc6-4* and *ppsmc6-5* mutants. The picture was taken after 1.5 months of growth. **h** Spontaneous mutagenesis in *APT* locus. The Fisher exact test statistic value 0.0418 indicates significant difference at $p < .05$

Single-cell gel electrophoresis (Comet) assay

Repair kinetics were estimated in 1d and 7d protonemata after bleomycin or MMS treatment. Tissue was either flash-frozen in liquid N_2 (repair t = 0) or left to recover in liquid BCDAT medium for the indicated repair times and then frozen. DSBs after bleomycin treatment were detected by a comet assay using neutral N/N protocol whereas SSBs after MMS treatment were detected with A/N protocol, which includes after lysis of nuclei a treatment with alkali to reveal breaks by unwinding the DNA double helix as described in (Angelis et al. 1999; Hola et al. 2013). Comets were stained with SYBR Gold (Molecular Probes/Invitrogen) and viewed in epifluorescence with a Nikon Eclipse 800 microscope and evaluated by the LUCIA Comet cytogenetic software (LIM Inc., Prague, Czech Republic).

The fraction of DNA in comet tails (% tail-DNA) was used as a measure of DNA damage. In each experiment, the % tail-DNA was measured at seven time points: 0, 3, 5, 10, 20, 60 and 180 min after the treatment and in control tissue without treatment. Measurements obtained in three, in case of *pprad51-1-2* two, independent experiments and totaling at least 300 comets analyzed per experimental point were plotted as % of remaining damage and statistically analyzed by Student's t-test.

Gene targeting assay (GT)

GT efficiencies were assessed after transformation with the APT based targeting construct pKA255 (Fig. 4). Vector pKA255 contains a 35S-Hygromycin marker ($Hygr^R$) flanked by 775bps 5′-homology fragment of *APT* locus (Pp3c8_16590V3.1) (position -766 - 9 across the start codon) and 622 bps 3′-homology fragment (658–1280) that were amplified from moss genomic DNA by PCR. Linear targeting fragment containing the 35S::HygrR flanked by genomic *PpAPT* sequences was amplified by PCR and delivered by PEG mediated transformation to WT and *ppnse4-4* and *ppsmc6-3* protoplasts (Liu and Vidali 2011). Transformed protoplasts of each line were spread on four Petri dishes with BCDAT medium overlaid with a cellophane disc. Regenerating protoplast were counted after 5 days on each Petri dish and then transferred to a new Petri dish with BCDAT medium supplemented with 30 mg/l Hygromycin. The relative transformation index (RTF) was calculated as a ratio of $Hygr^R$ resistant transformants vs total number of regenerating protoplasts. Cellophane discs with $Hygr^R$ transformants were transferred onto plates with BCDAT medium containing 5 µM 2-fluoroadenine (2-FA) to detect GT events in APT. 2-FA resistant ($2\text{-}FA^R$) colonies were counted after 3 weeks. Frequency of GT is expressed as the ratio of $2\text{-}FA^R$ vs $Hygr^R$ colonies. The experiment was repeated three times and statistically analyzed using the Fisher exact test.

Integration of pKA255 was checked by PCR in six randomly picked $2\text{-}FA^R$ clones of each line with external gene primers *868* and *727* and selection cassette primers *1023* and *1024* and integration borders were confirmed by sequencing with primers *862*, *857*, *1259* and *1258* (Supplementary Table S1).

Phylogenetic analysis

The Arabidopsis protein sequence of AtSMC6A (AT5G07660.1), AtSMC6B (AT5G61460.1), AtNSE4A (AT1G51130.1) and AtNSE4B (AT1G51130.1) retrieved from TAIR (https://doi.org/10.1002/dvg.22877) were used for Blast search against *P. patens* genome database Phytozome v12.1 (Goodstein et al. 2012). The search identified single copy locus for both *P. patens* NSE4 (Pp3c27_130V3.1) and SMC6 (Pp3c11_11190V3.1). *Homo sapiens* HsNSE4A (NP_060085.2), HsNSE4B (NP_001008395.1) and HsSMC6 (NP_001135758.1), *Schizosaccharomyces pombe* SpNSE4 (NP_001018837.1) and SpSMC6 (NP_587906.1), *Saccharomyces cerevisie* ScNSE4 (NP_010178.1) and ScSMC6 (NP_013487.1) protein sequences were retrieved from the National Center for Biotechnology Information.

Mid-point rooted phylogenetic trees of SMC6 and NSE4 were obtained from Phylogeny.fr server (Dereeper et al. 2008) using MUSCLE algorithm for protein alignment (Edgar 2004), Gblocks for the alignment refinement and phylogeny software PhyML for the phylogenetic trees building (Guindon et al. 2010) (Fig. 1).

Statistical analysis

Three biological repeats were conducted for each experiment. Statistical significance between two samples was analyzed by two-tailed Student's t-test.

Results and discussion

Generation and analysis of *ppnse4* and *ppsmc6* mutants

Using *A. thaliana* protein sequences for Blast search the *P. patens* genome (Phytozome v12.1) we identified single copy loci for *NSE4* (Pp3c27_130V3.1) and of *SMC6* (Pp3c11_11190V3.1).

Firstly, we tried to generate knock-out mutants by recombinational replacement of entire or partial N' or C' sections of both genes, but after several attempts we were not able to recover any viable clones. Based on similar observations in *S. pombe* (Lehmann et al. 1995; Vondrova et al. 2020) and *A. thaliana* (Diaz et al. 2019; Yan et al. 2013) we concluded

that in haploid *P. patens NSE4* and *SMC6* are also essential genes and their deletion is lethal. This is why the issue was addressed by modulating the gene expression through lowering the transcript levels with targeted binding of dCas9. We obtained stable dCas9_sgRNA transformants by targeting the *NSE4* promotor (Fig. 2a) and *SMC6* hinge region (Fig. 2d). It was not possible to recover any stable dCas9 transformant by targeting the *SMC6* promotor or ATPase Walker A region.

Three randomly selected lines of *NSE4*$^{-}$ (*ppnse4-2,3* and *4*) and of *SMC6*$^{-}$ (*ppsmc6-3,4,5*) were analyzed for remaining presence of the respective transcripts (*NSE4*, Fig. 2b and *SMC6*, Fig. 2e) by qRT-PCR. In this study we used *ppnse4-4* with 15% and *ppsmc6-3* with 40% reduction of transcript abundance, respectively, both represent the lowest quantities of transcripts in rescued lines. The phenotype of *ppnse4-4* did not manifest any obvious deviation from WT, whereas *ppsmc6-3* growth was both reduced, and developmentally aberrant, the plants failing to develop gametophores (Fig. 2g). The cut-off for manifestation of the *SMC6*$^{-}$ phenotype lay under 71% of relative transcript level as manifested by formation of gametophores above this level in *ppsmc6-4*, *ppsmc6-5* and WT (Fig. 2g). The decrease of transcript levels was repeatedly confirmed in both lines over a period of several months.

Frequencies of spontaneously emerging 2-FA^{R} colonies in population of regenerated protoplasts were used as a marker for evaluation of the mutator phenotype at the *PpAPT* locus. In comparison to WT and *ppnse4-4*, only *ppsmc6-3* manifested a strong mutator phenotype (Fig. 2h). We assume that mutation of the SMC5/6 complex interferes with error-free repair of intrinsic lesions of whatever origin by disturbing DNA tethering.

Recovery from bleomycin and MMS treatment depends on PpSMC6

To characterize DNA repair defects in *ppnse4-4* and *ppsmc6-3* mutants we compared their growth-responses to lesions like DSBs induced by radiomimetic bleomycin, small alkylation adducts induced by MMS and DNA helix distortion by photo adducts induced by UVC irradiation. These lesions represent blocks for DNA replication and are removed, repaired or bypassed by various error-free as well as error-prone pathways. The sensitivity was tested after acute treatment for 1 h as the ability of the tissue to recover.

In response to the treatment with bleomycin or MMS, sensitivities of *ppnse4-4* and *ppsmc6-3* substantially differed. After exposure to 30 µg bleomycin/ml and 30 mM MMS *ppsmc6-3* explants did not recover at all, while *ppnse4-4* still retain about 50% viability (Fig. 3a, b). It is interesting that whereas the sensitivity of *ppnse4-4* was similar to WT in response to MMS (Fig. 3b), it was remarkably resistant to bleomycin treatment (Fig. 3a). This phenomenon is evidently a common feature of *ppnse4* mutants (see *ppnse4-3* on Fig. 2c) that deserves further clarification. Nevertheless, the response to bleomycin and MMS suggests that formation of the NSE4 bridge and the circular form of the SMC5/6 complex is not inevitably necessary to offset toxic effects of DNA lesions and so enable cell survival, but availability of the complex itself and so far, undisclosed functions are necessary for cell survival. The response of *ppnse4-4* and *smc6-3* to UVC-irradiation indicated their sensitivity to induced lesions, when *ppsmc6-3* remained the most vulnerable.

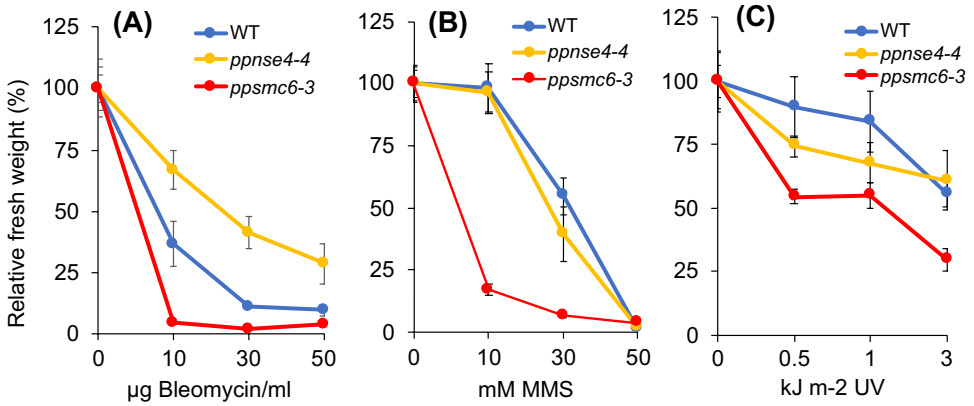

Fig. 3 Growth-responses of protonemata of *P. patens* WT, *ppnse4-4* and *ppsmc6-3* to 1 h treatment with bleomycin (**a**), MMS (**b**) or UVC-irradiation (**c**). After treatment, the explants were incubated on drug-free BCDAT medium under standard growth conditions for 3 weeks. For each experimental point the weight of treated plants collected from two replicas was normalized to the weight of untreated plants and plotted as relative fresh weight, which was set as a default to 100. Error bars indicate SD

DSB repair is impaired in *nse4* and *smc6*

DSB repair is severely inhibited in both *ppnse4-4* and *ppsmc6-3* lines. This is the case in the 1d-regenerated lines in which the enhanced preponderance of mitotically active apical cells results in rapid repair of DSBs, and also in the 7d-regenerated lines in which the repair of DNA-DSBs occurs more slowly (Fig. 4a, c). In this respect they closely parallel previously reported repair defects in *A. thaliana* mutant *atmim* (*atsmc6b*) (Kozak et al. 2009). SMC6B was suggested to participate in the NHEJ pathway due to absence of the initial rapid phase of repair kinetic that is characteristic of NHEJ repair (Goodarzi et al. 2010). To ascertain the repair pathway in which SMC6 is involved, we compared *ppnse4-4* and *ppsmc6-3* with the cNHEJ mutant *ppku70* and the HR mutant *pprad51-1-2*. Statistical analysis showed that their repair kinetic differs from both, *pprad51-1-2* (1d $p < 0.01$; 7d $p < 0.05$) and *ppku70* (1d and 7d $p < 0.05$). This result is in accord with the conclusion from *A. thaliana* that SMC5/6 is involved in tethering DNA strands during alternative NHEJ, distinct from cNHEJ. For tethering DNA and participation in DSB repair, bridging of ATPase heads of SMC5/6 heteroduplex by the kleisin NSE4 is critical. This is supported by the observation that the weak, 15% decrease of *NSE4* transcripts results in the same extent of repair deficit as 40% decrease of *SMC6* transcripts.

MMS does not induce DSBs detectable by comet assay and repair of SSBs in WT and all mutants is completely abolished (Fig. 4b, d). This is in contrast with repair of bleomycin induced SSBs when in WT 50% of breaks are already removed after 3 h (Hola et al. 2013).

Gene targeting is attenuated in the *nse4* and *smc6* mutants

Transformation frequencies were determined at every stage of selection and GT efficiencies as the frequency of 2-FA resistant plants among hygromycin resistant integrative transformants. Targeting vector pKA255 (Fig. 5a) was designed to disrupt the *PpAPT* gene across the second

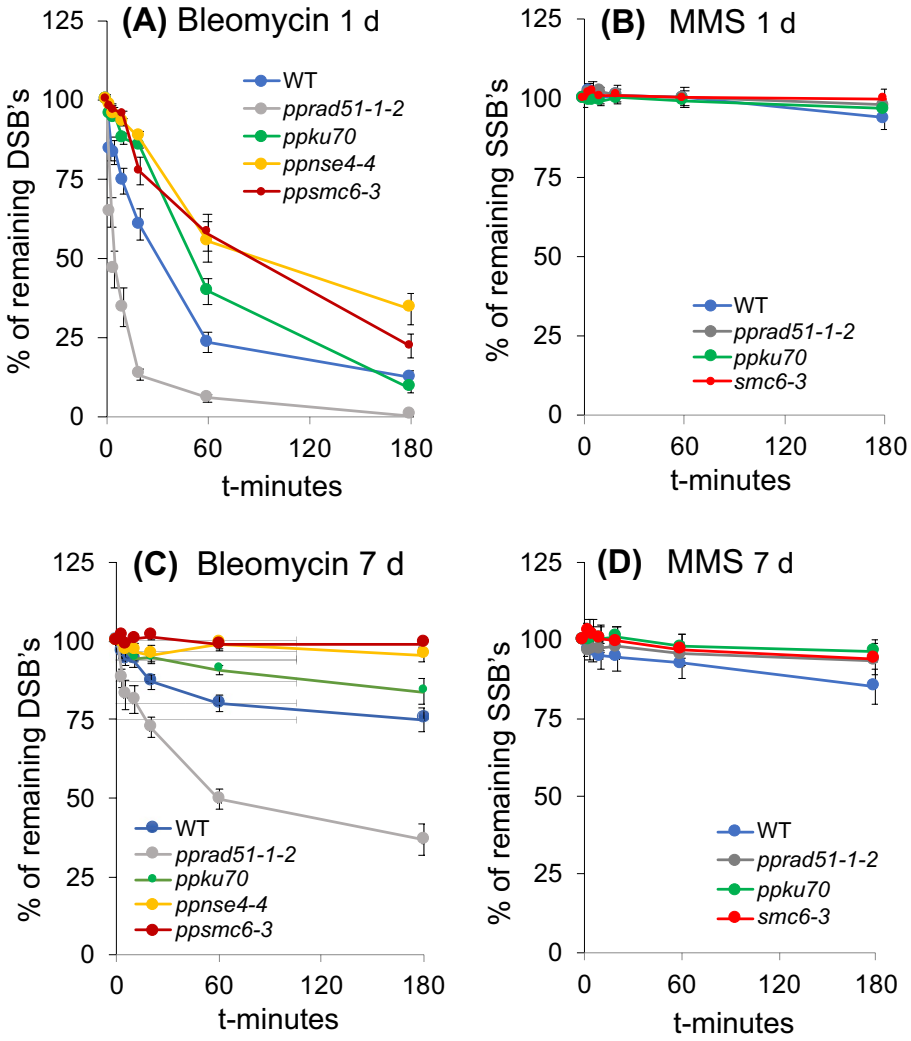

Fig. 4 DSB and SSB repair kinetics determined by comet assay in 1d or 7d tissue of WT (blue), *ppnse4,4* (orange), *ppsmc6-3* (red), *ppku70* (green) and *pprad51-1-2* (gray) mutants. Protonemata, which regenerated for 1 (**a**, **b**) or 7 (**c**, **d**) days after subculture were treated with 30 µg bleomycin/ml (**a**, **c**) or 30 mM MMS (**b**, **d**) for 1 h and repair kinetics was measured as % of DSBs (**a**, **c**) or SSB (**b**, **d**) remaining after the 0, 3, 5, 10, 20, 60 and 180 min of repair recovery. Maximum damage is normalized as 100% at t = 0 for all lines. Error bars indicate SD

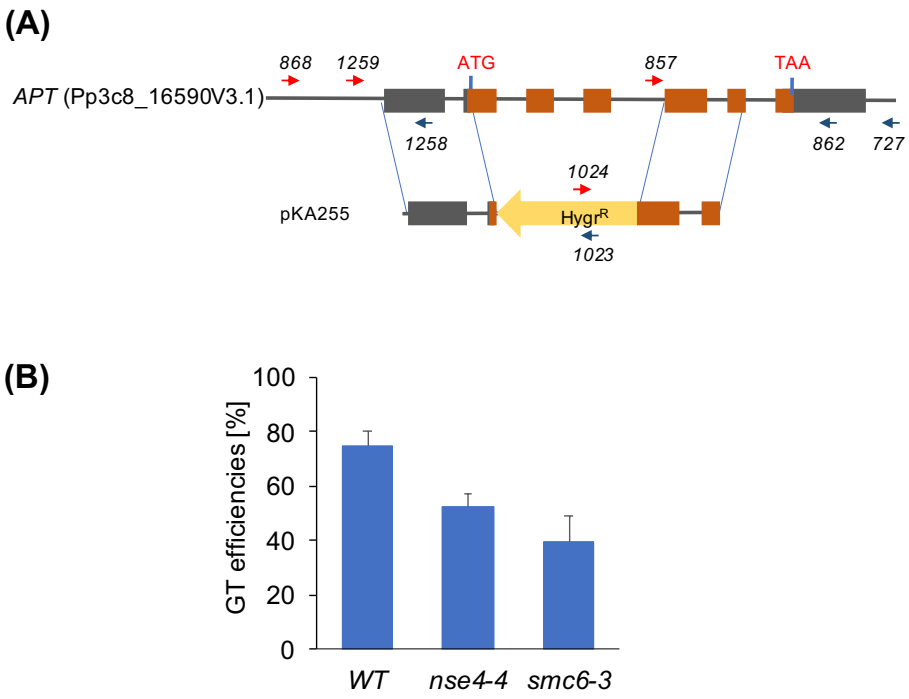

Fig. 5 GT assay. (**a**) Schematic drawing of *APT* locus and of targeting construct pKA255. The boxes represent exons and the gray shading indicate UTR regions. Arrows mark position of primers used to genotype and sequence the plants by PCR (Supplementary Table S1). (**b**) GT efficiencies in *ppnse4-4* and *ppsmc6-3* in comparison to WT. Error bars indicate SD. (**c**) Comparison of transformation and GT efficiencies. RTF [in ‰] is the frequency of $Hygr^R$ transgenic clones in the whole regenerating protoplasts population, $Hygr^R$ and $2\text{-}FA^R$ indicate total and average ± SD resistant clones determined from 3 independent experiments, each of them performed in triplicate, GT [in %] express the frequency of $2\text{-}FA^R$ resistant among the population of $Hygr^R$ transgenic clones. Differences between WT and mutants were compared using Fisher's exact test

(C)

Genotype	RTF [‰]	$Hygr^R$	$2\text{-}FA^R$	GT [%]
WT	2.96 ± 1.1	169 (33.8 ± 7.7)	126 (25.2 ± 5.2)	75
nse4-4	1.51 ± 0.5	165 (18.3 ± 4.4)	87 (9.7 ± 2.0)	53
smc6-3	1.07 ± 0.4	48 (8.0 ± 2.8)	19 (3.2 ± 0.7)	40

exon site (229–339) previously identified as a mutation hotspot (Hola et al. 2013, 2015) and provide transformants with Hygromycin resistance. The initial efficiency of transformation depends on the genotype and decreases in the range from 2.96×10^{-3} for WT, 1.51×10^{-3} for *ppnse4-4* to 1.07×10^{-3} for *ppsmc6-3*. Gene targeting efficiency calculated as the ratio of $2\text{-}FA^R$ clones to primary $Hygr^R$ transformants also depends on genotype and decreases from 75% for WT, 53% for *ppnse4-4* to 40% for *ppsmc6-3*, respectively (Fig. 5c). PCR analysis of randomly selected $2\text{-}FA^R$ plants of each genotype was performed to assess accuracy of integration and revealed that in two $2\text{-}FA^R$ transformants of each line insert borders had accurate insertion without mutation at both ends of insert. This experiment shows that SMC5/6 complex is involved in transformation and plays an important role during targeted insertion. If we assume targeted integration as closely connected with HR, our results also show that SMC5/6 complex participates in the process of HR.

Conclusion

In this study we used haploid *P. patens* cultivated on rich BCDAT medium as chloronemata with varying proportions of cells arrested at the G2/M border to study the role of the SMC5/6 complex in DNA repair. We generated lines with modified expression of essential *NSE4* and *SMC6* genes by CRISPR/dCas9. SMC5/6 in circular form is indispensable for DSB repair presumably by NHEJ, but not the cNHEJ pathway, as is illustrated by the same repair kinetic of the *smc6* and kleisin *nse4* mutants compared with that of the *ku70* mutant. Nevertheless, the repair dependent on NSE4 is not essential for cell survival after bleomycin and MMS treatment as the incurred damage can be offset by alternative repair mechanisms. The question remains which functions and qualities of SMC5/6 enable survival of *nse4* after bleomycin or MMS treatment, but are disturbed in *smc6*, or are the observed

differences just consequence of different degrees of *NSE4* and *SMC6* expression? In addition, the decreased rate of GT and mutator phenotype of *smc6* points to possible role of the SMC5/6 complex also in error-free HR. It is evident that further studies are needed to decipher complex functioning of SMC5/6, its interactions and roles of core and associated components in the DNA repair and cell survival (Vondrova et al. 2020).

Acknowledgements The research was supported by the Czech Science Foundation (project 20-05095S) and by the Ministry of Education, Youth and Sports of the Czech Republic under the project COST (LTC17047). We acknowledge Jan Paleček, MU Brno, Czech Republic for helpful discussions and critical reading of the manuscript and A.C.Cuming, CPS-UoL, UK for improving the manuscript.

Author contributions MH and KJA designed the research, analyzed data and wrote the manuscript. RV, MH and KJA conducted the research.

Compliance with ethical standards

Conflict of interests The authors declare no conflicts of interest.

References

Angelis KJ, Dusinska M, Collins AR (1999) Single cell gel electrophoresis: detection of DNA damage at different levels of sensitivity. Electrophoresis 20:2133–2138

Angelis KJ, Kozák J, Vágnerová R, Holá M (2015) DNA repair in plants studied by comet assay. Front Genet. https://doi.org/10.3389/conf.fgene.2015.01.00067

Dereeper A et al (2008) Phylogeny.fr: robust phylogenetic analysis for the non-specialist Nucleic. Acids Res 36:W465–W469. https://doi.org/10.1093/nar/gkn180

Diaz M, Pecinka A (2018) Scaffolding for repair: understanding molecular functions of the SMC5/6 complex. Genes. https://doi.org/10.3390/genes9010036

Diaz M et al (2019) The SMC5/6 complex subunit NSE4A is involved in DNA damage repair and seed development. Plant Cell 31:1579–1597. https://doi.org/10.1105/tpc.18.00043

Edgar RC (2004) MUSCLE: a multiple sequence alignment method with reduced time and space complexity. BMC Bioinform 5:113. https://doi.org/10.1186/1471-2105-5-113

Gaillard C, Moffatt BA, Blacker M, Laloue M (1998) Male sterility associated with APRT deficiency in *Arabidopsis thaliana* results from a mutation in the gene APT1. Mol Gen Genet 257:348–353. https://doi.org/10.1007/s004380050656

Goffova I et al (2019) Roles of RAD51 and RTEL1 in telomere and rDNA stability in Physcomitrella patens. Plant J 98:1090–1105. https://doi.org/10.1111/tpj.14304

Goodarzi AA, Jeggo P, Lobrich M (2010) The influence of heterochromatin on DNA double strand break repair: getting the strong, silent type to relax. DNA Repair 9:1273–1282. https://doi.org/10.1016/j.dnarep.2010.09.013

Goodstein DM et al (2012) Phytozome: a comparative platform for green plant genomics. Nucleic Acids Res 40:D1178–D1186. https://doi.org/10.1093/nar/gkr944

Guindon S, Dufayard JF, Lefort V, Anisimova M, Hordijk W, Gascuel O (2010) New algorithms and methods to estimate maximum-likelihood phylogenies: assessing the performance of PhyML 3.0. Syst Biol 59:307–321. https://doi.org/10.1093/sysbio/syq010

Hola M, Kozak J, Vagnerova R, Angelis KJ (2013) Genotoxin induced mutagenesis in the model plant *Physcomitrella patens*. Biomed Res Int 2013:535049. https://doi.org/10.1155/2013/535049

Hola M, Vagnerova R, Angelis KJ (2015) Mutagenesis during plant responses to UVB radiation. Plant Physiol Biochem 93:29–33. https://doi.org/10.1016/j.plaphy.2014.12.013

Hu B et al (2005) Qri2/Nse4, a component of the essential Smc5/6 DNA repair complex. Mol Microbiol 55:1735–1750. https://doi.org/10.1111/j.1365-2958.2005.04531.x

Ju L et al (2013) SMC6 is an essential gene in mice, but a hypomorphic mutant in the ATPase domain has a mild phenotype with a range of subtle abnormalities. DNA Repair 12:356–366. https://doi.org/10.1016/j.dnarep.2013.02.006

Kamisugi Y et al (2012) MRE11 and RAD50, but not NBS1, are essential for gene targeting in the moss *Physcomitrella patens*. Nucleic Acids Res 40:3496–3510. https://doi.org/10.1093/nar/gkr1272

Kamisugi Y, Whitaker JW, Cuming AC (2016) The transcriptional response to DNA-double-strand breaks in *Physcomitrella patens*. PLoS ONE 11:e0161204. https://doi.org/10.1371/journal.pone.0161204

Knight CD, Cove DJ, Cumming AC, Quatrano RS (2002) Molecular plant biology vol 2. Practical approach, vol 2. Oxford University Press, Oxford

Kozak J, West CE, White C, da Costa-Nunes JA, Angelis KJ (2009) Rapid repair of DNA double strand breaks in *Arabidopsis thaliana* is dependent on proteins involved in chromosome structure maintenance. DNA Repair 8:413–419. https://doi.org/10.1016/j.dnarep.2008.11.012

Lehmann AR, Walicka M, Griffiths DJ, Murray JM, Watts FZ, McCready S, Carr AM (1995) The rad18 gene of *Schizosaccharomyces pombe* defines a new subgroup of the SMC superfamily involved in DNA repair. Mol Cell Biol 15:7067–7080. https://doi.org/10.1128/mcb.15.12.7067

Li G, Zou W, Jian L, Qian J, Deng Y, Zhao J (2017) Non-SMC elements 1 and 3 are required for early embryo and seedling development in Arabidopsis. J Exp Bot 68:1039–1054. https://doi.org/10.1093/jxb/erx016

Liu YC, Vidali L (2011) Efficient polyethylene glycol (PEG) mediated transformation of the moss *Physcomitrella patens*. J Vis Exp. https://doi.org/10.3791/2560

Menand B, Calder G, Dolan L (2007) Both chloronemal and caulonemal cells expand by tip growth in the moss *Physcomitrella patens*. J Exp Bot 58:1843–1849. https://doi.org/10.1093/jxb/erm047

Palecek JJ (2018) SMC5/6: multifunctional player in replication. Genes. https://doi.org/10.3390/genes10010007

Palecek J, Vidot S, Feng M, Doherty AJ, Lehmann AR (2006) The Smc5-Smc6 DNA repair complex. bridging of the Smc5-Smc6 heads by the KLEISIN, Nse4, and non-Kleisin subunits. J Biol Chem 281:36952–36959. https://doi.org/10.1074/jbc.m608004200

Pfaffl MW (2004) Quantification strategies in real-time PCR. A-Z of Quantitative PCR. International University Line, La Jolla

Qi LS, Larson MH, Gilbert LA, Doudna JA, Weissman JS, Arkin AP, Lim WA (2013) Repurposing CRISPR as an RNA-guided platform for sequence-specific control of gene expression. Cell 152:1173–1183. https://doi.org/10.1016/j.cell.2013.02.022

Rensing SA et al (2008) The Physcomitrella genome reveals evolutionary insights into the conquest of land by plants. Science 319:64–69. https://doi.org/10.1126/science.1150646

Rensing SA, Goffinet B, Meyberg R, Wu SZ, Bezanilla M (2020) The Moss Physcomitrium (Physcomitrella) patens: a model organism for non-seed plants. Plant Cell 32:1361–1376. https://doi.org/10.1105/tpc.19.00828

Schaefer DG et al (2010) RAD51 loss of function abolishes gene targeting and de-represses illegitimate integration in the moss *Physcomitrella patens*. DNA Repair 9:526–533. https://doi.org/10.1016/j.dnarep.2010.02.001

Schleiffer A, Kaitna S, Maurer-Stroh S, Glotzer M, Nasmyth K, Eisenhaber F (2003) Kleisins: a superfamily of bacterial and eukaryotic SMC protein partners. Mol Cell 11:571–575. https://doi.org/10.1016/s1097-2765(03)00108-4

Schween G, Gorr G, Hohe A, Reski R (2003) Unique tissue-specific cell cycle in Physcomitrella. Plant Biol 5:50–58. https://doi.org/10.1055/s-2003-37984

Trouiller B, Schaefer DG, Charlot F, Nogue F (2006) MSH2 is essential for the preservation of genome integrity and prevents homeologous recombination in the moss *Physcomitrella patens*. Nucleic Acids Res 34:232–242. https://doi.org/10.1093/nar/gkj423

Trouiller B, Charlot F, Choinard S, Schaefer DG, Nogue F (2007) Comparison of gene targeting efficiencies in two mosses suggests that it is a conserved feature of Bryophyte transformation. Biotechnol Lett 29:1591–1598. https://doi.org/10.1007/s10529-007-9423-5

Vondrova L, Kolesar P, Adamus M, Nociar M, Oliver AW, Palecek JJ (2020) A role of the Nse4 kleisin and Nse1/Nse3 KITE subunits in the ATPase cycle of SMC5/6. Sci Rep 10:9694. https://doi.org/10.1038/s41598-020-66647-w

Yan S et al (2013) Salicylic acid activates DNA damage responses to potentiate plant immunity. Mol Cell 52:602–610. https://doi.org/10.1016/j.molcel.2013.09.019

Zelkowski M et al (2019) Arabidopsis NSE4 proteins act in somatic nuclei and meiosis to ensure plant viability and fertility. Front Plant Sci 10:774. https://doi.org/10.3389/fpls.2019.00774